Radiation Shielding

References

1- M. Abdou, *Radiation Considerations for Superconducting Magnets*, Journal of Nuclear Materials, 72 (1978) 147-167 (Handout No. 12)

2- First Part of Handout No. 9 on *Radiation Damage in Superconducting Magnet Materials*

3- Handout No. 13

Types of Shielding in Fusion Reactor

- **Bulk Shield** (Surrounding the blanked to protect vacuum vessel and superconducting magnets.
- **Penetration Shield** (Around penetrations, e.g. natural beams, vacuum ducts)
- **Biological** (Reactor building walls, typically concrete; protect personnel in central rooms and outside.

Bulk Shield

This is a large component of fusion reactor. It is outside the blanket and inside the vacuum vessel.

Topics to be covered

1- Shield material composition

2- Radiation damage to superconducting magnet materials

3- Optimization of inboard blanket/shield thickness

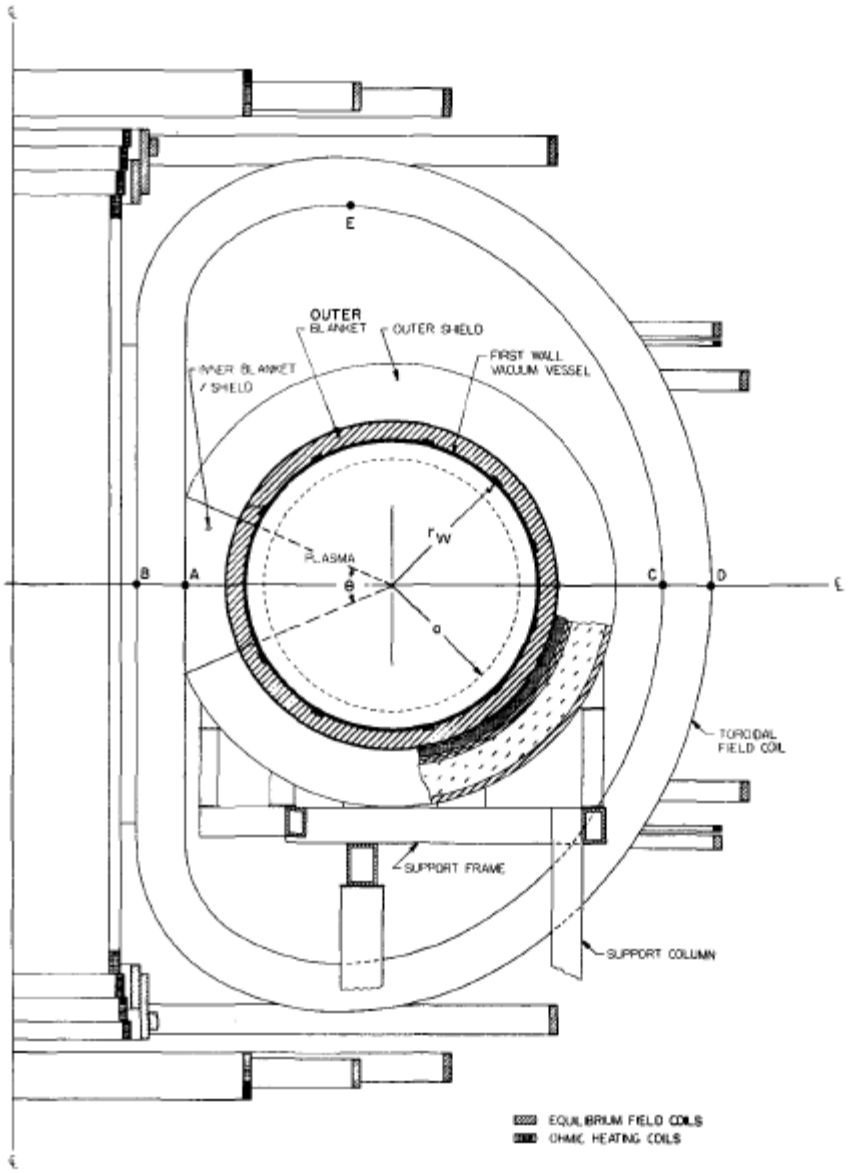

Fig. 4. A simplified vertical cross section of a representative tokamak with circular plasma.

II. Shield Composition

A considerable fraction of the neutrons leaking from the blanket have kinetic energies above a few MeV. A basic requirement therefore of the shielding material is to have a large attenuation coefficient for high energy neutrons. Inevitably, this has to be a material of moderate or large mass number since inelastic scattering is the most efficient mechanism for reducing the energies of high energy neutrons. Furthermore, light materials such as water, LiH, and lithium have small total cross sections at high energies when compared with heavy materials. Stainless steel and lead have relatively large total cross sections above 3 MeV and the average secondary neutron energy per inelastic collision at 14 MeV is 2.2 and 2.5 MeV in lead and iron, respectively. Both materials are available, relatively inexpensive, and a great deal of knowledge about their characteristics exists. Below the inelastic threshold, however, these materials are no longer effective and a light material should be present. Borated water is efficient and is almost cost free. However, the presence of water in the same system with a high-temperature liquid metal increases significantly the hazard of accidental energy release. Graphite is an alternative choice. In addition, to minimize the gamma emission from radiative capture reactions, it is essential to use a sufficient amount of B^{10} which has a large (n,α) cross section for low energy neutrons and is associated with only soft gamma (.5 MeV) emission (compared with a strong line at 7.6 MeV in the capture gamma ray spectrum for iron). Boron carbide (B_4C) has been used in control rod applications in fission reactors and seems an excellent choice for neutron moderation and absorption at low energies. With its theoretical density, B_4C has a high content of B^{10} of 0.0217 atoms/cm^3. No significant radioactive decay products are formed in B_4C irradiation but helium production is large. However, if B_4C is used in the shield with only 80% of the theoretical density, the swelling problem due to the excessive helium production can be tolerated. Boral (50% B_4C and 50% Al) is another good choice.

Based on the above discussion, a mixture of stainless steel and boron carbide, or of lead and B_4C, or a combination of the three materials are reasonable choices and further investigation is needed to find the optimum composition and shield depth for an overall low cost. For this purpose, a fixed composition and configuration of the blanket coupled to a shield for which the parameters are to be varied as shown in figure 1 is considered. The blanket consists of a 1 cm first wall, 42 cm of 95% Li plus 5% structure, 20 cm stainless steel, and 7 cm of 95% Li plus 5% structure. The first wall and blanket structure is niobium in the following calculations but the results in the shield are insensitive to this choice. The extra 7 cm of lithium at the outer face of the reflector region was introduced to meet the cooling requirements of the reflector and inner regions of the shield. As preliminary criteria, the attenuation required in the blanket and shield should be roughly 10^6. This requirement can be satisfied by approximately 70 cm of stainless steel plus boron carbide following the blanket described above. As a starting point, figure 1 in which the blanket is followed by a one meter shield was considered as a reference design for investigating various aspects of the shield design. Six cases for the composition of the shield were considered; 70% SS plus 30% B_4C (design 114), 70% Pb plus 30% B_4C (design 115), 35% SS plus 35% Pb plus 30% B_4C (design 116), 100% SS (design 117), 85% Pb + 15% B_4C (design 118), and 50% Pb + 50% B_4C (design 119), where percentages are by volume. Neutronics and photonics calculations were carried out for the six designs. It has been shown[1] that the convergence of the discrete ordinates results for such a system are achieved by S_8 and S_4 overestimates the leakage by 10 to 15%. In order to reduce the cost for these calculations, S_4 was used. The comparison is not significantly affected by the difference between S_4 and S_8. Cylindrical geometry and the P_3 approximation of the scattering anisotropy were used in all calculations.

The energy leakage, L_{TE}, is plotted against the distance from the inner boundary of the shield for designs 114 through 117 in fig. 2 and for designs

115, 118, and 119 in figure 3. L_{TE}, is the sum of the neutron energy leakage, L_{nE}, and the gamma energy leakage, $L_{\gamma E}$, where L_{nE} is defined in the multigroup representation at any surface of a one-dimensional cylinder as

$$L_{nE}(r) = 2\pi r \cdot \sum_{g} E_{ng}(r)\, J_{ng}(r) \qquad (1)$$

where J_{ng} is the (net) neutron current density at the surface in energy group g, and E_{ng} is approximated by the midpoint energy of group g. Similar definitions apply for gammas with the subscript γ replacing n. Since the energy deposition in the magnet by neutrons and photons streaming out of the shield increases, in general, with the neutron and photon energies we find it more meaningful in comparing the performance of various shield compositions to compare the "energy" rather than the "number" attenuations.

The results in figures 2 and 3 show that L_{TE} varies exponentially with the spatial variable, r, i.e.

$$L_{TE}(r) = L_{TE}(r_0)\, e^{-\mu_t (r - r_0)} \qquad (2)$$

where μ_t (with or without the subscript) is the total energy attenuation coefficient. Similar results were found for both the neutron and gamma fluxes i.e.

$$L_{nE}(r) = L_{nE}(r_0)\, e^{-\mu_n (r - r_0)} \qquad (3)$$

$$L_{\gamma E}(r) = L_{\gamma E}(r_0)\, e^{-\mu_\gamma (r - r_0)} \qquad (4)$$

The energy attenuation coefficients μ_n, μ_γ, and μ_t obtained for the six designs discussed above are given in table I. Several conclusions can be reached from examining the attenuation curves of figures 2 and 3 and the energy attenuation coefficients in table I: 1- Comparison of L_{TE} for designs 114, 115 and 116 shows that stainless steel has considerably better attenuation characteristics than lead if both are mixed with a fair amount of light material. 2- Comparison of L_{TE} for designs 114 and 117 shows that the presence of B_4C (or an alternative) is necessary. At the end of a one meter shield the total energy leakage from a 100% stainless steel shield is about two orders of magnitude higher than that from a shield consisting of 70% SS plus 30% B_4C. This is mainly due to two causes. B_4C is better than SS at attenuating neutrons below about 2 MeV. In addition, in the absence of B^{10}, neutrons slowed down eventually get absorbed in radiative capture reactions in stainless steel increasing the gamma energy production. 3- Figure 3 which compares L_{TE} for 85% Pb + 15% B_4C, 70% Pb + 30% B_4C, and 50% Pb + 50% B_4C shows that increasing the volume percentage of B_4C to 50% (and probably higher) improves the attenuation considerably. If other light materials such as graphite or water are used, the optimal volume percentages are usually much less (roughly 30%) than that for B_4C. 4- Although lead is more efficient in attenuating gamma radiation, we found that using stainless steel does not increase the gamma energy leakage, $L_{\gamma E}$, appreciably. Furthermore, table I shows that μ_γ is greater in stainless steel-B_4C than in Pb-B_4C mixtures. These results can be explained as follows. The photons in the shield come primarily from gammas produced by neutron interactions in the shield rather than by penetration from the blanket. Stainless steel attenuates fast neutrons quickly in the first few mean free paths, thus the photons produced have a long distance in which to be absorbed. In addition, the gamma energy leakage in the outer regions is affected most by the gammas produced in these regions. The secondary gamma production in deeper regions of a SS-B_4C shield is significantly lower than that in the same regions of the Pb-B_4C shield.

III. Optimization of Shield Thickness

Increasing the thickness of the shield increases its cost and the magnet

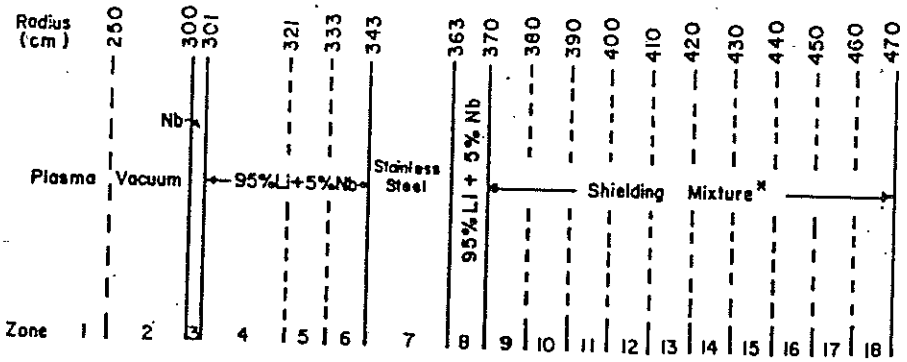

* Shielding mixture varies in this series of designs as follows:

Design 114: 70% SS+30% B_4C, Design 115: 70% Pb + 30 % B_4C

Design 116: 35% SS + 35% Pb + 30% B_4C, Design 117: 100% SS

Design 118: 85% Pb + 15 % B_4C, Design 119: 50% Pb + 50% B_4C

Fig. 1. Reference design for shield calculations

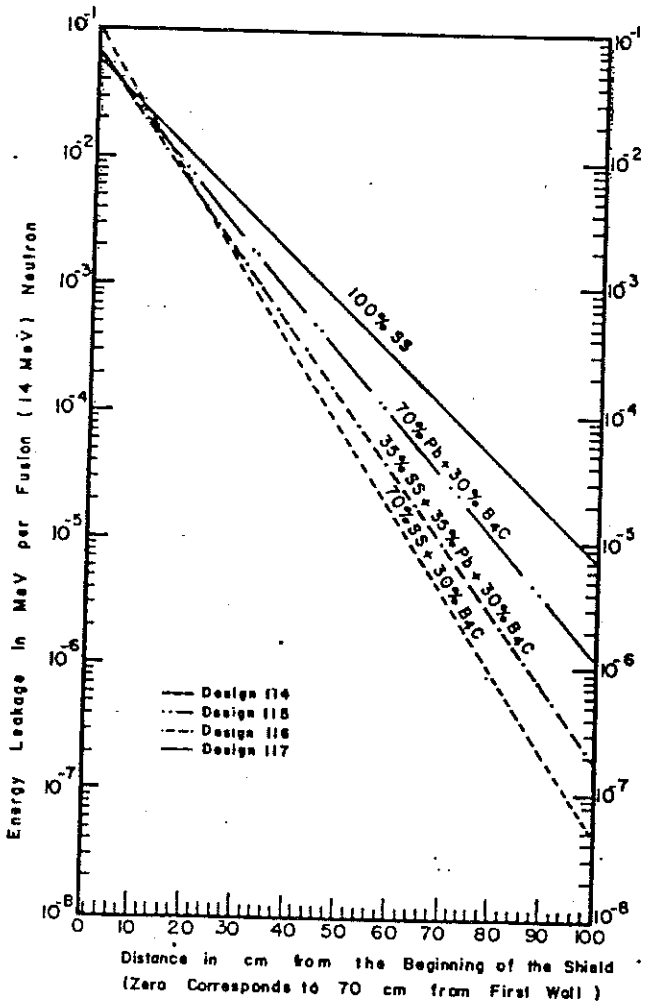

Fig. 2. Energy leakage versus depth in various shield compositions

Table I

Neutron, Gamma, and Total Energy Attenuation Coefficients* for Various Shield Compositions

Design ID	114	115	116	117	118	119
Shield Composition (all percentages are by volume)	70% SS + 30% B_4C	70% Pb + 30% B_4C	35% Pb + 35% SS + 30% B_4C	100% SS	85% Pb + 15% B_4C	50% Pb + 50% B_4C
Neutron Energy Attentuation Coefficient, μ_n (cm^{-1})	0.1438	0.1113	0.1282	0.1022	0.0977	0.1161
Gamma Energy Attenuation Coefficient, μ_γ (cm^{-1})	0.1466	0.1160	0.1320	0.0828	0.1008	0.1190
Total Energy Attenuation Coefficient, μ_t (cm^{-1})	0.1445	0.1113	0.1283	0.0902	0.0976	0.1161

*obtained by fitting the energy attenuation curves to exponentials (see Text)

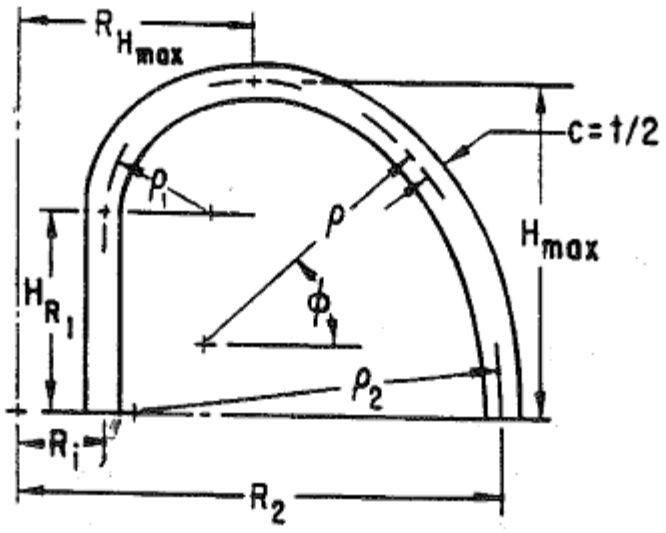

Figure 3. Geometric Parameters for a Constant-Tension Coil

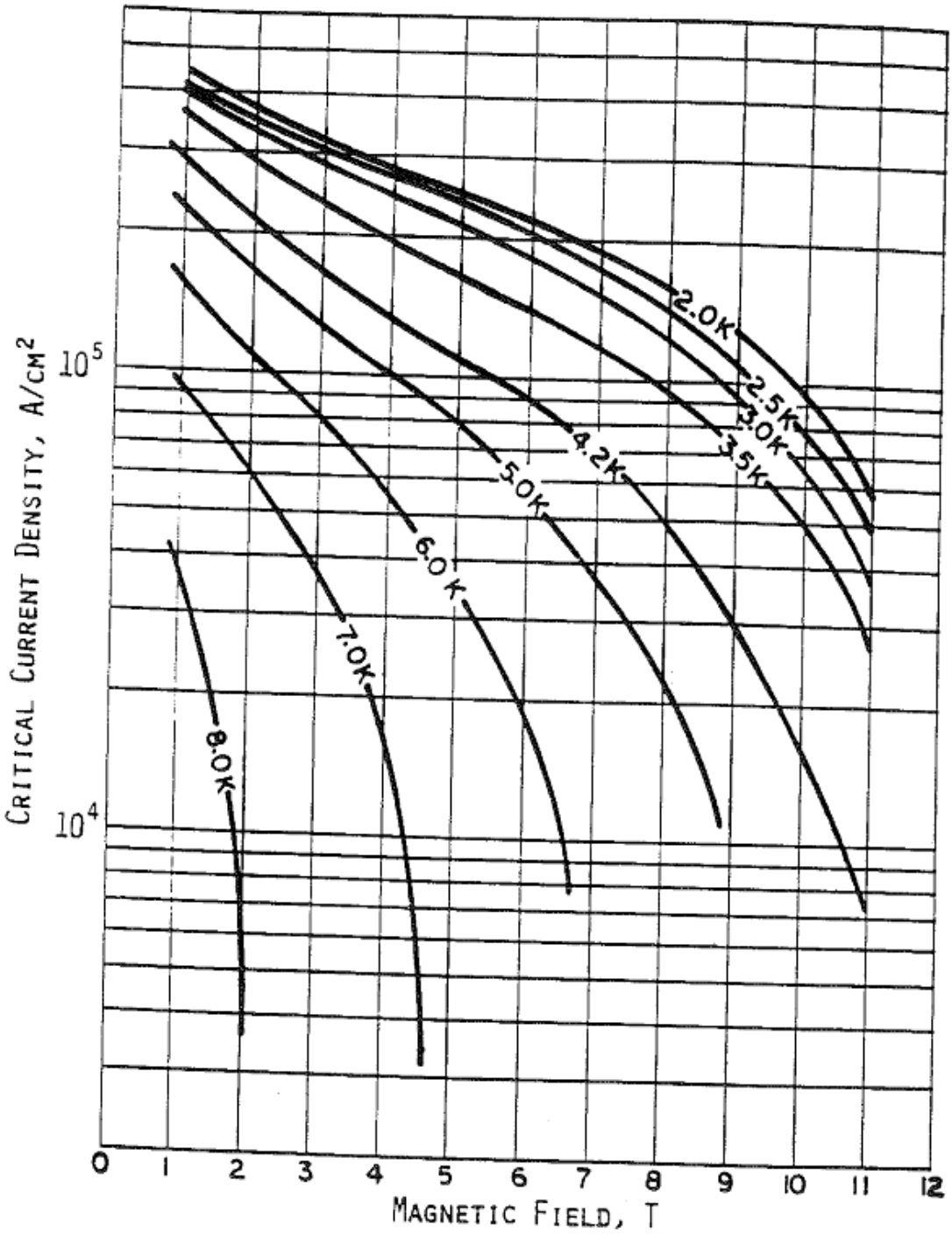

Figure 2. J-H Curve for NbTi Versus Temperature

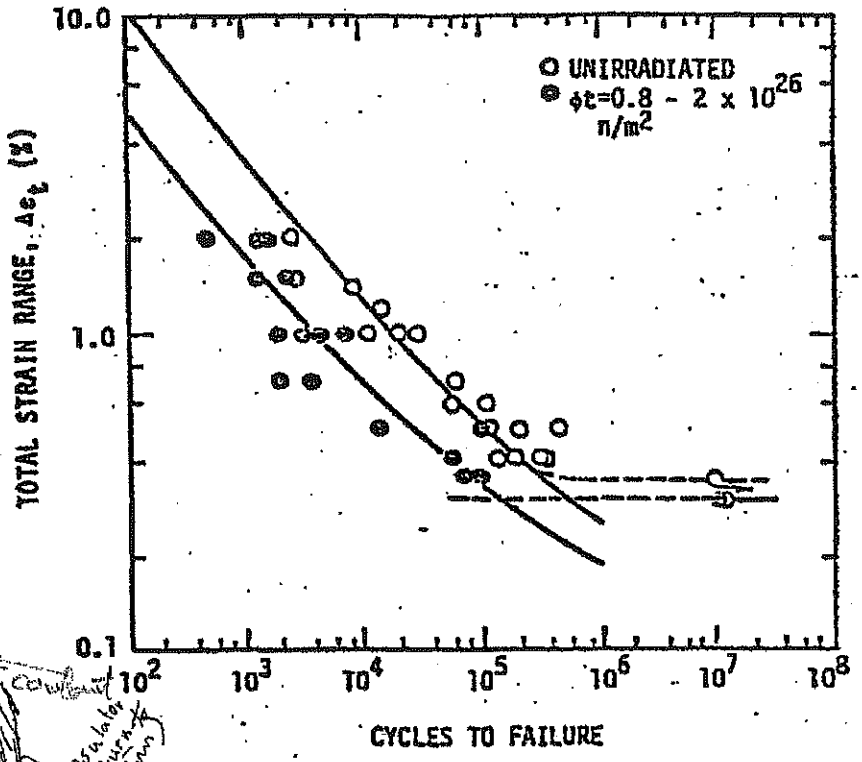

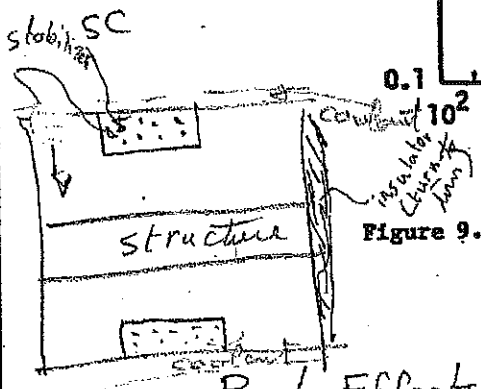

Figure 9.4.6. Fatigue Life of 20% Cold-Worked Type 316 Stainless Steel Irradiated at 430°C and Tested at the Irradiation Temperature (200-1,000 appm He, 5-15 dpa).

Rad. Effects in Superconducting magnets

Superconducting magnet components are adversely affected by radiation, also. The effect of neutron radiation on the superconductor itself is to diminish the superconducting region of current density-temperature-magnetic field phase space. The critical current density of Nb_3Sn has been observed to ~~deteriorate severely~~ change above ~1.5×10^{-3} dpa (3×10^{22} n/m^2). The effect is much less pronounced for NbTi, with a decrease of less than a factor of 2 being observed at fluences up to 10^{24} n/m^2. These data are shown in Figure 9.4.7.

J_c in Superconductors

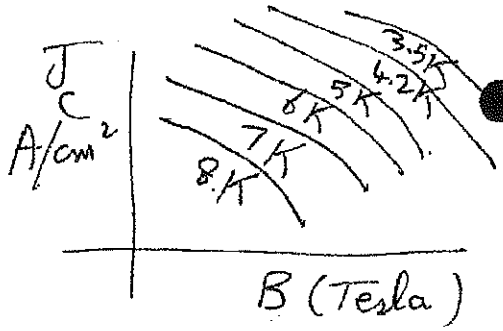

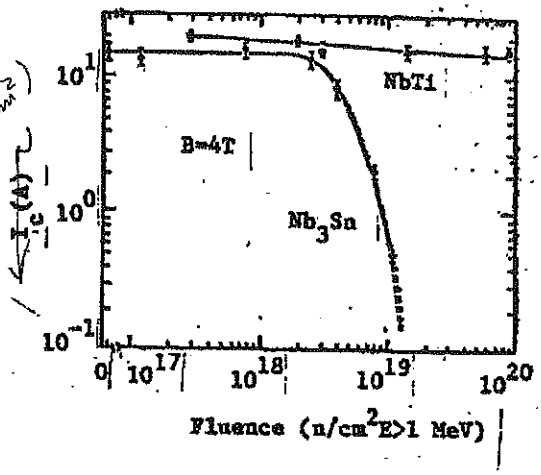

Figure 9.4.7. Effect of Neutron Irradiation on the Critical Current in NbTi and Nb_3Sn.

ρ in normal conductors

The resistance of normal conductors, which are used for cryogenic stability, at 4.2 K increases dramatically with dpa, as illustrated in Figure 9.4.8.

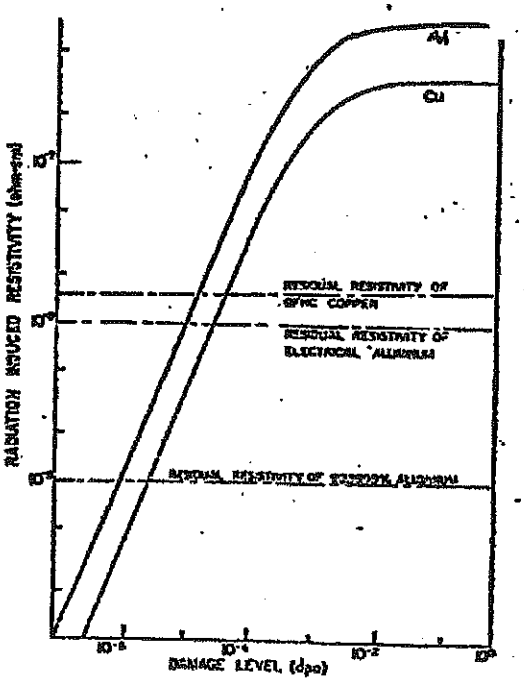

Figure 9.4.8. Radiation Induced Resistivity of Copper and Aluminum.

$2-5 \times 10^9$ rad
1 rad $\sim 10^9$ n/cm^2 $\sim 10^{13}$ n/m^2

The organic insulators that are used in superconducting magnets have been observed to physically deteriorate from neutron damage in the range $2-5 \times 10^{22}$ n/m^2. Inorganic insulators, on the other hand, retain their physical properties up to damage in excess of 10^{25} n/m^2. However, the inorganic insulators are brittle.

Solid Breeders

There are indications that neutron radiation-induced microstructural change in granular solid breeding materials (see Section 10.1) may significantly reduce the tritium release properties. Tritium trapping at radiation-induced defects could be significant. Radiation-induced sintering could lead to reduction in porosity, which would reduce the tritium migration. The size of the basic grains could grow under radiation, leading to reduced tritium diffusion out of the grains in which it is produced.

swelling

9.5 Radioactivity

Many of the new isotopes produced by nuclear transmutations following neutron capture (e.g. (n,γ), (n,α), (n,p), (n,2n)) are unstable and will, over a period of time, decay by the emission of a charged particle. The resulting isotope may itself be unstable and undergo further decay, thus leading to a so-called decay chain. The nuclide densities of the isotopes in a given decay chain are described by the set of equations

Follow Handwritten notes

$$\frac{dN_i(\vec{r},t)}{dt} = -\left(\lambda_i + \bar{\sigma}_i \bar{\phi}(\vec{r})\right) N_i(\vec{r},t) + \sum_{j \neq d}^{J} \left(\lambda_j a_{j-i} + \bar{\sigma}_{j-i} \bar{\phi}(\vec{r})\right) N_j(\vec{r},t),$$

$$i = 1, \ldots, J$$

Here, λ_i is the radioactive decay constant for isotope i and $a_{j \to i}$ is the probability that the decay of isotope j leads to isotope i (e.g. if the

Optimization of Inboard Blanket / Shield Thickness in Tokamak

Tradeoffs between:

- Reactor size, reactor power, magnetic field, etc.
- Protection of S.C. Magnet

MOTIVES FOR LARGER BLANKET/SHIELD THICKNESS

Shield Function: radiation protection of S.C. magnet

$$\phi_m \sim \phi_w e^{-\mu \Delta_{BS}^{i}}$$

ϕ_w = flux at first wall (fixed by design)

μ = attenuation coefficient (fixed by shielding composition)

Magnet Protection

(1) refrigeration power requirements

(2) change in superconductor J_c, T_c

(3) radiation-induced resistivity in stabilizer

(4) change in mechanical and dielectric properties of insulators

MOTIVE FOR SMALLER BLANKET/SHIELD THICKNESS

A. Effect on Reactor Power

$$P \sim B_t^4$$

B_t = magnetic field at the plasma center

$$B_t = B_m\left(1 - \frac{1}{A_w} - \frac{\Delta^i_{BS}}{R}\right)$$

B_m = maximum magnetic field (at coil windings)

A_w = aspect ratio $= a/R$

R = major radius

Δ^i_{BS} = blanket/shield thickness on the inside of the torus.

$$\frac{B_t}{B_m} = \frac{R - a - \Delta_v - \Delta_w - \Delta_s - \Delta_{vv}}{R}$$

MOTIVES FOR SMALLER BLANKET/SHIELD THICKNESS

B. Effects on TF and OH Magnetic Field Requirements

$$B_t = B_m\left(1 \pm \frac{1}{A_w} - \frac{\Delta^i_{BS}}{R}\right)$$

For a fixed reactor power, B_t is fixed.

Increasing Δ^i_{BS} increases B_m.

TF magnet cost $\sim B_m^2$ (also technology requirements).

Increase Δ^i_{BS} → increases B_m.

Increase TF magnet thickness t_m.

Increase support cylinder thickness t_s.

Reduces central core radius, R_v.

$$R_v = R - \Delta^i_{BS} - t_m - t_s$$

Decrease R_v → increases OH field.

$$B_{OH} \sim \frac{1}{R_v^2}$$

Cost of OH power supply $\sim \frac{1}{R_v^4} \sim \left(\Delta^i_{BS}\right)^4$

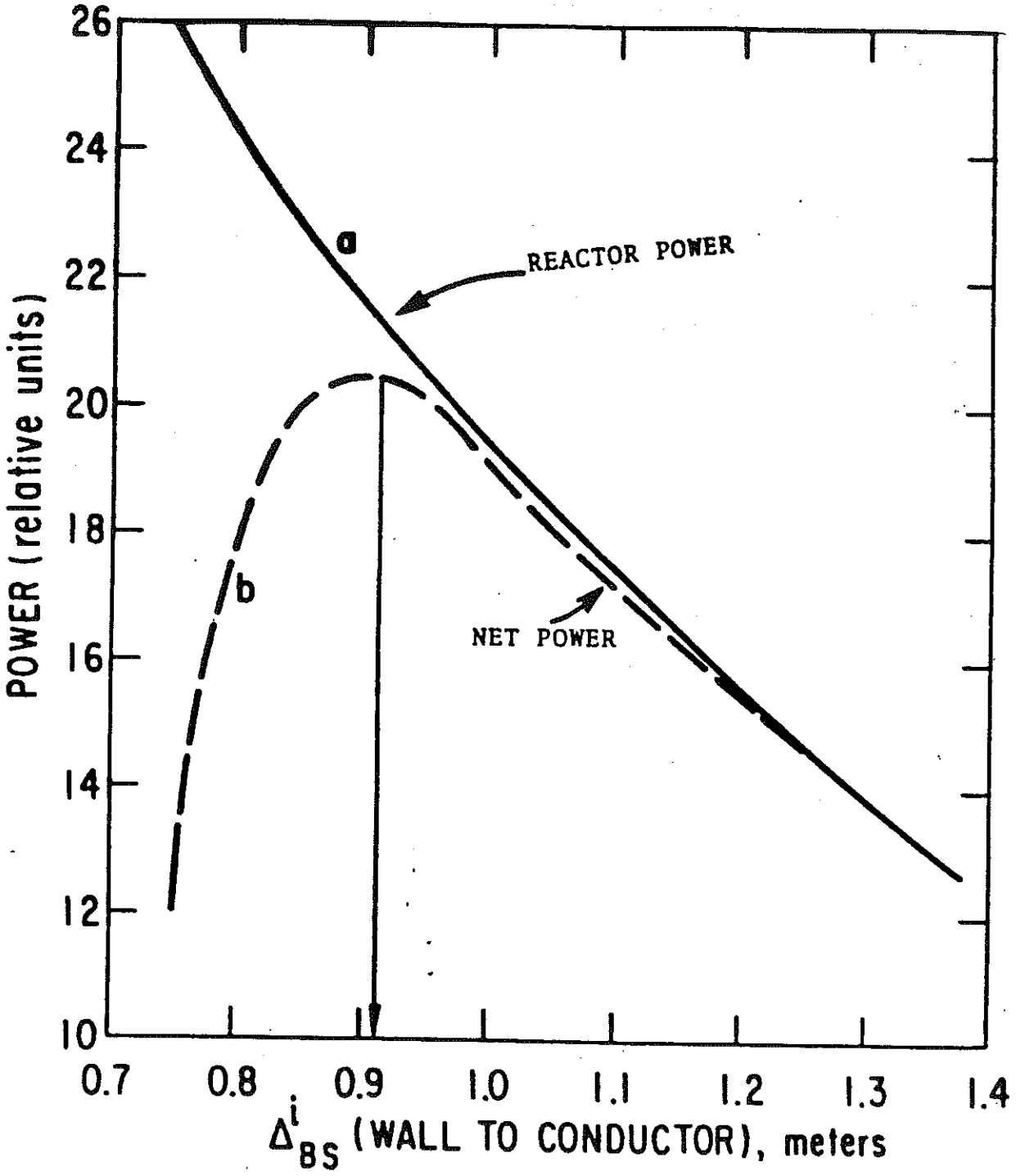
26
24
22
20
18
16
14
12
10
POWER (relative units)
a
REACTOR POWER
b
NET POWER
0.7
0.8
0.9
1.0
1.1
1.2
1.3
1.4
Δ^{i}_{BS} (WALL TO CONDUCTOR), meters

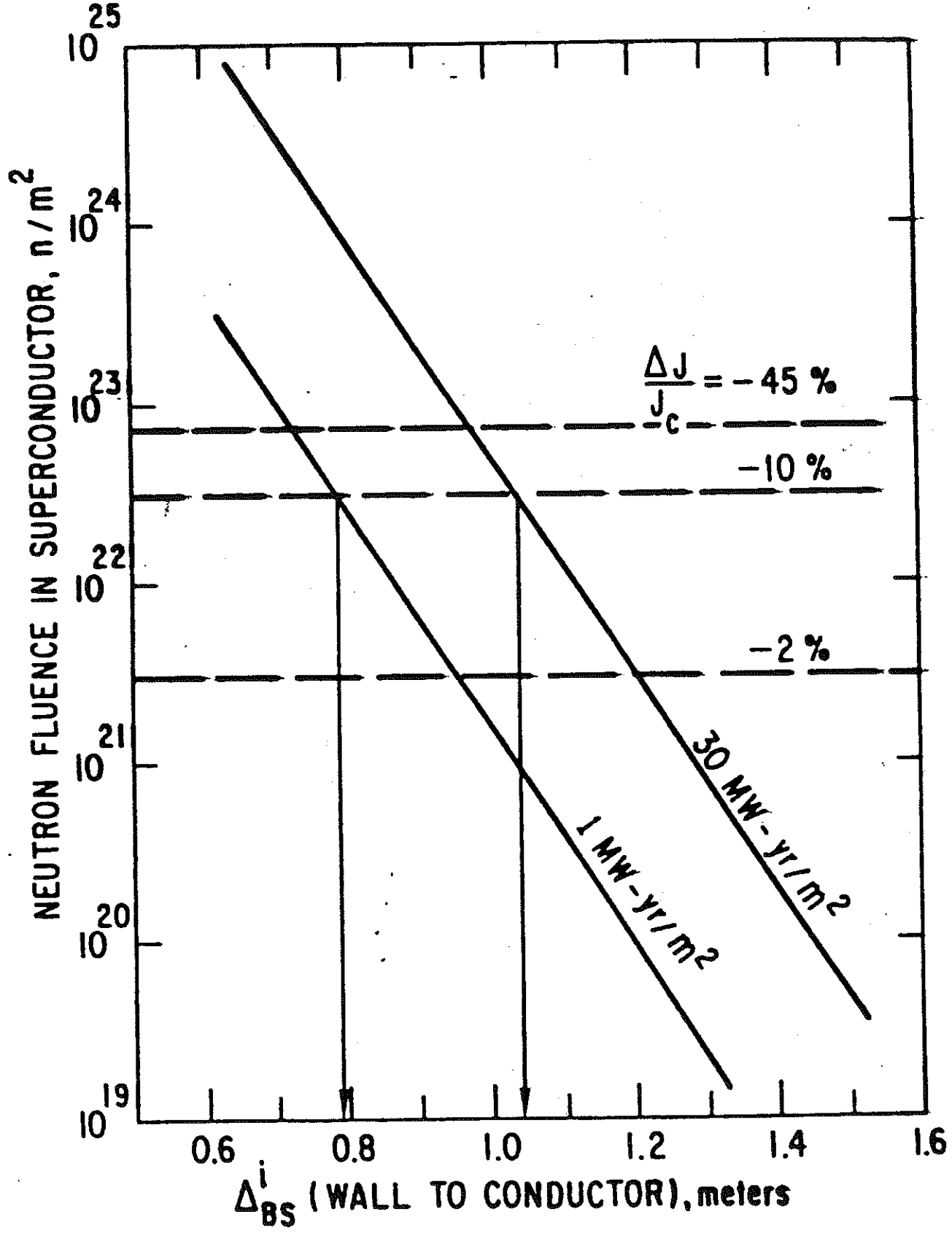
NEUTRON FLUENCE IN SUPERCONDUCTOR, n/m²
10²⁵
10²⁴
10²³
10²²
10²¹
10²⁰
10¹⁹
ΔJ/Jc = −45 %
−10 %
−2 %
30 MW-yr/m²
1 MW-yr/m²
0.6
0.8
1.0
1.2
1.4
1.6
Δ^i_BS (WALL TO CONDUCTOR), meters

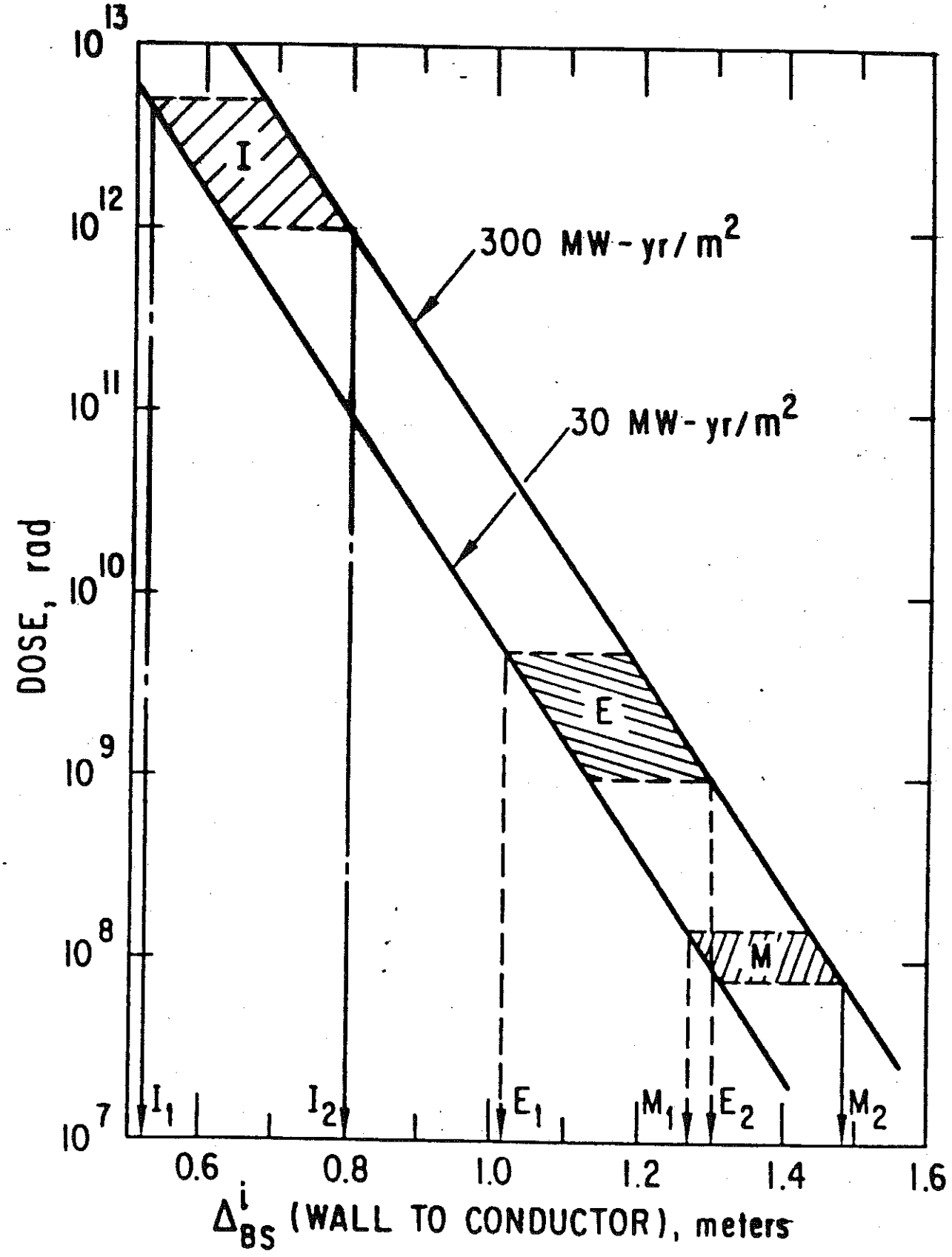
10^{13}
10^{12}
10^{11}
10^{10}
10^{9}
10^{8}
10^{7}
DOSE, rad
I
300 MW-yr/m^2
30 MW-yr/m^2
E
M
I_1
I_2
E_1
M_1
E_2
M_2
0.6
0.8
1.0
1.2
1.4
1.6
Δ^i_{BS} (WALL TO CONDUCTOR), meters

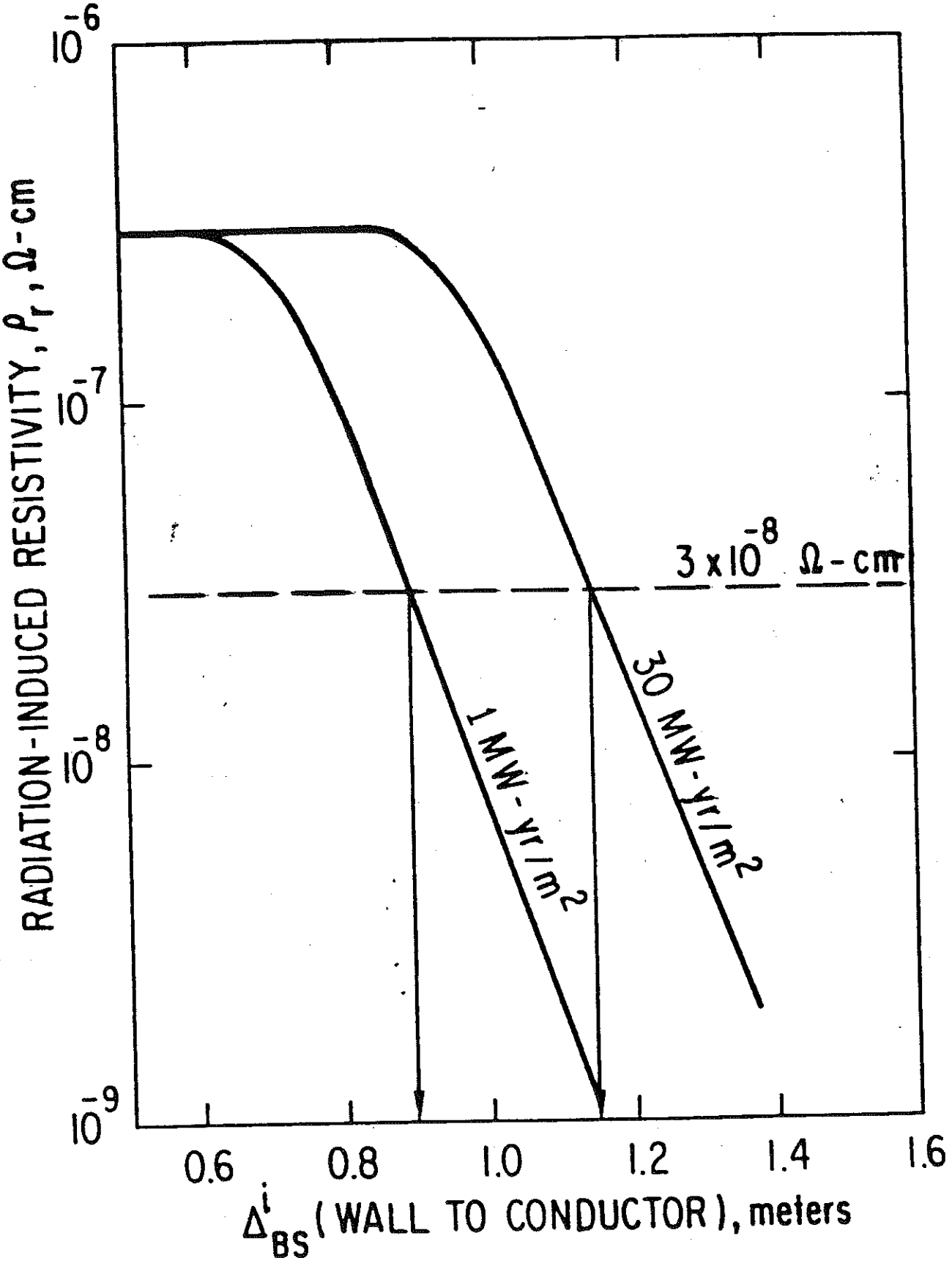
RADIATION-INDUCED RESISTIVITY, ρ_r, Ω-cm
10^{-6}
10^{-7}
10^{-8}
10^{-9}
3×10^{-8} Ω-cm
1 MW-yr/m^2
30 MW-yr/m^2
0.6
0.8
1.0
1.2
1.4
1.6
Δ^i_{BS} (WALL TO CONDUCTOR), meters

DEFINITIONS

Neutron Wall Loading, P_w

$$P_w = J_w E_0$$

J_w = neutron current of fusion neutrons at the first wall

E_0 = fusion neutron energy (14.06 MeV for D-T cycle)

P_w is measured in units of MW/m^2 ($\sim$1-5)

(1 MW/m^2) corresponds to $J_w = 4.43 \times 10^{17}$ $n/m^2 s$

For a given reactor, the neutron flux at the magnet $\propto P_w$.

Integral Neutron Wall Loading, I_w

$$I_w = P_w \cdot t_0 \cdot F$$

t_0 = operation period

F = plant capacity factor ($\sim$0.7-0.9)

I_w is measured in units of $MW\text{-}yr/m^2$

For a given reactor the neutron fluence at the magnet is $\propto I_w$.

$$\text{Fluence} = \int_{n/cm^2} \phi t = \phi \cdot F \cdot t_{op} \quad \left(\phi : n/cm^2 \cdot s\right)$$

ASP - 3.0, KAPPA - 1.00
DEITY - 0.00, 0-3.0, PW - 3.0
RMAJ IS SWEPT, TDOWN - 80

WALL MATERIAL IS VANADIUM, T - 650

LEGEND
□ - 6.00E+00
○ - 7.00E+00
△ - 8.00E+00
+ - 9.00E+00

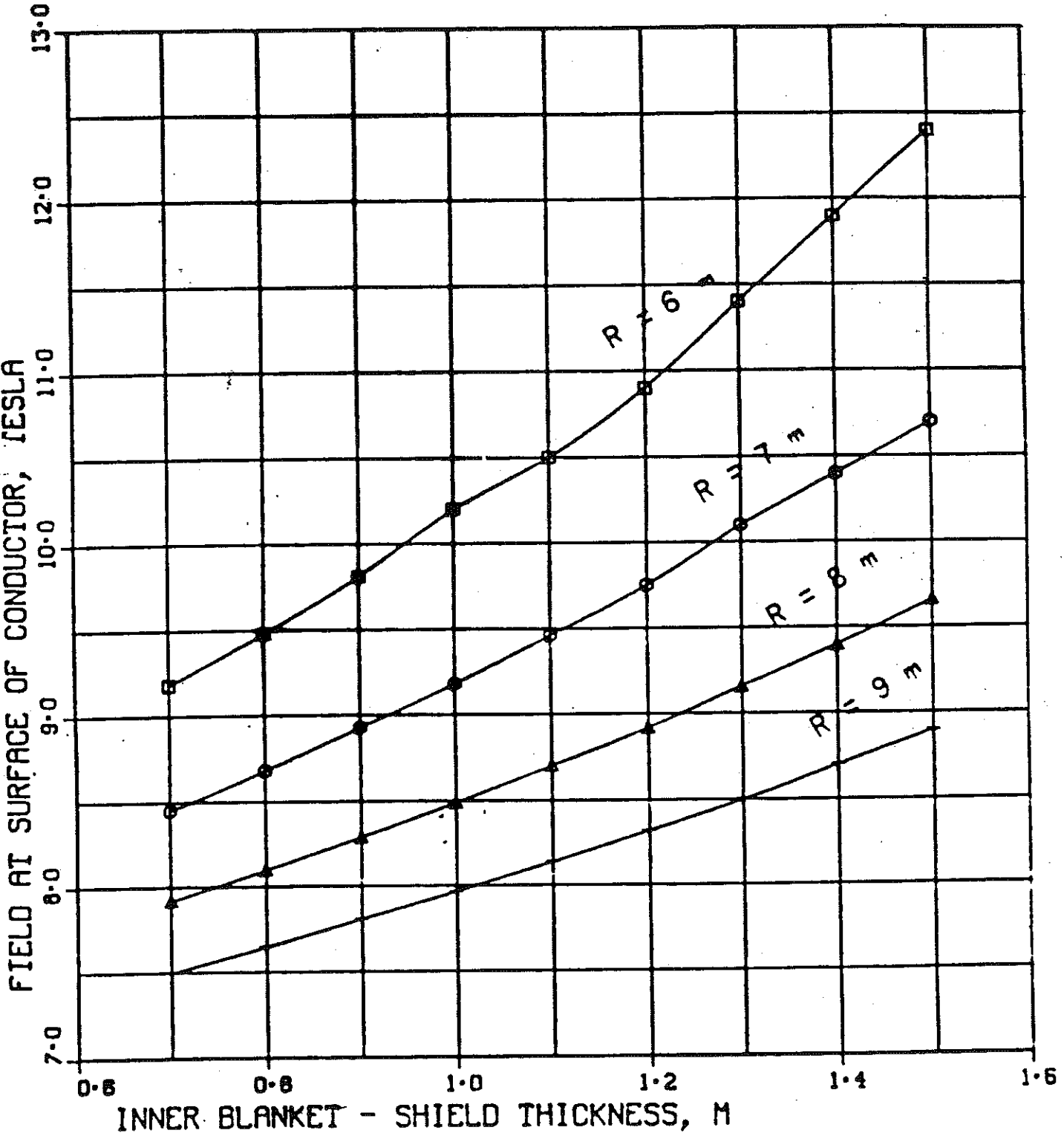

ASP = 3.0, KAPPA = 1.00
DELTA = 0.00, Q=3.0, PW = 3.0
RMAJ IS SWEPT, IDOWN = 80

WALL MATERIAL IS VANADIUM, T = 650

LEGEND
□ - 6.00E+00
○ - 7.00E+00
△ - 8.00E+00
+ - 9.00E+00

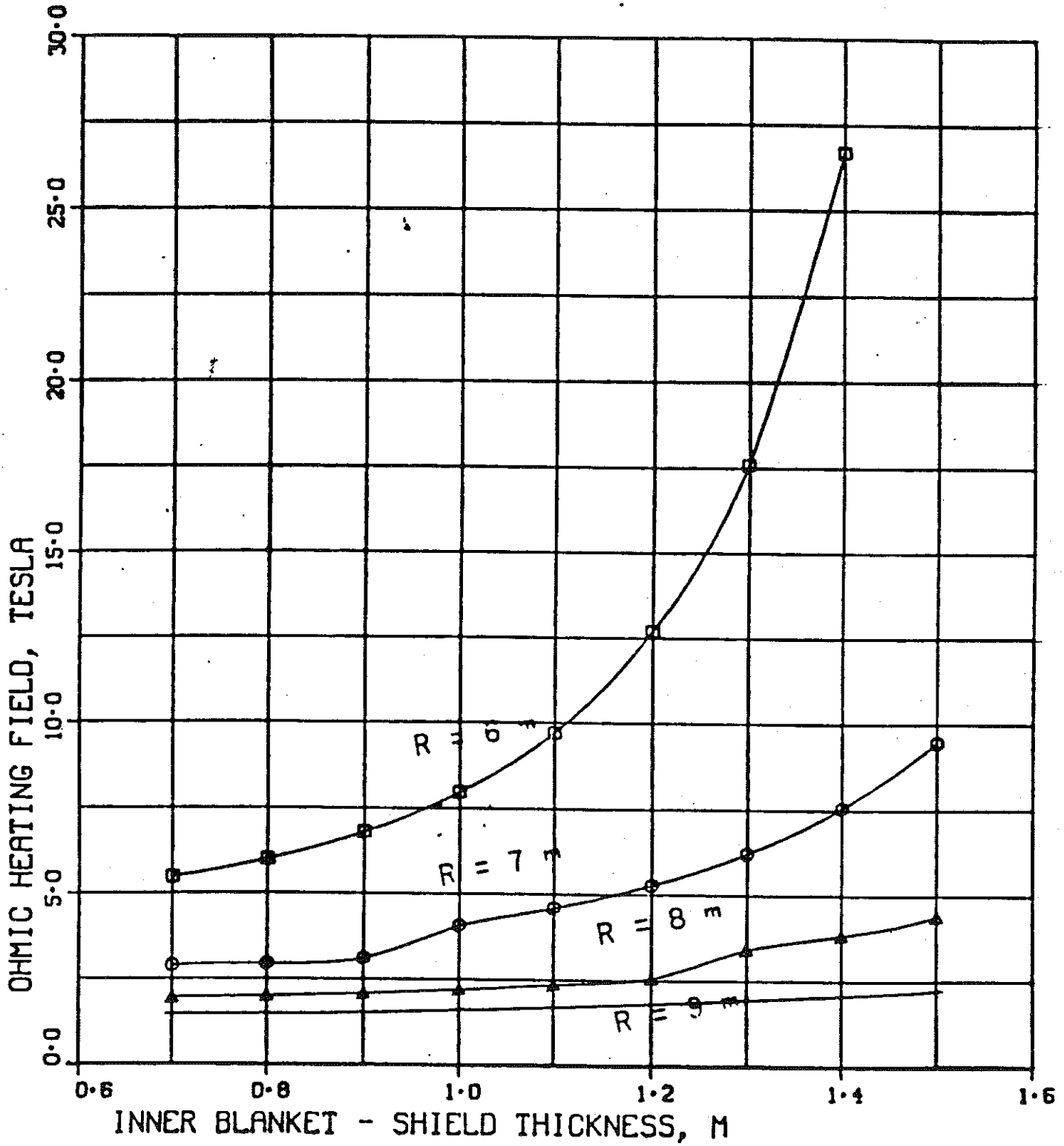

[illegible] TOKAMAK SYSTEMS STUDY (UNITS MKS AND KEV)

ASP = 3.0, KAPPA = 1.00
DELTA = 0.00, Q=3.0, PW = 3.0
RMAJ IS SWEPT, IDOWN = 80

WALL MATERIAL IS VANADIUM, T = 650